

Analysis of Multi-Element Airfoil High Lift Improvement by Efficient Upper Surface Suction

Veldhuis, Leo; van Craenenbroeck, Jorik

DOI

[10.2514/6.2017-1211](https://doi.org/10.2514/6.2017-1211)

Publication date

2017

Document Version

Accepted author manuscript

Published in

55th AIAA Aerospace Sciences Meeting

Citation (APA)

Veldhuis, L., & van Craenenbroeck, J. (2017). Analysis of Multi-Element Airfoil High Lift Improvement by Efficient Upper Surface Suction. In *55th AIAA Aerospace Sciences Meeting: Grapevine, Texas* Article AIAA 2017-1211 American Institute of Aeronautics and Astronautics Inc. (AIAA). <https://doi.org/10.2514/6.2017-1211>

Important note

To cite this publication, please use the final published version (if applicable).
Please check the document version above.

Copyright

Other than for strictly personal use, it is not permitted to download, forward or distribute the text or part of it, without the consent of the author(s) and/or copyright holder(s), unless the work is under an open content license such as Creative Commons.

Takedown policy

Please contact us and provide details if you believe this document breaches copyrights.
We will remove access to the work immediately and investigate your claim.

Analysis of multi-element airfoil high lift improvement by efficient upper surface suction

Leo Veldhuis*, Jorick van Craenenbroeck†
Delft University of Technology

In this paper we address a preliminary assessment of the performance effects of upper surface suction for multi-element airfoils. For this purpose new boundary layer closure relations were defined and implemented in a viscous-inviscid interaction code, denoted MatSESSuction, which was based on the well known MSES code. After a validation of the code an analysis of several multi-element airfoils was made that exhibit a significant lift reduction due to wake bursting beyond certain critical flap deflection angles. The application of suction close to the trailing edge of the main element shows that an efficient (i.e. low power consumption) system may be developed that increases the lift of typical high lift systems on modern transport aircraft.

I. Introduction

Even if high lift systems are complex and rather heavy they are still indispensable to ensure optimal cruise performance of the aircraft with an acceptable take-off and landing performance. However, a definitive trend towards lower complexity high lift systems is ongoing and new methods to arrive at lighter and simpler high lift systems are actively investigated. One of the methods that has already proven to be able to increase high lift performance is boundary layer suction (BLS). The main disadvantage of boundary layer suction however is that it is a form of active boundary layer (BL) control with often high power requirements. In an attempt to reduce the power requirements and minimize the weight penalty of a boundary layer suction system, systems that use an already existing low-pressure area in the engine¹ are interesting to pursue. Along the same line of reasoning a BLS system can be envisaged that is driven by a ‘naturally occurring’ low pressure zone, such as the low pressure zone near the flap end vortex. However, the pressure difference that can be expected from are expected to be very low, certainly not in the order of magnitude that is necessary for a typical BLS system. Therefore, the requirements needed to obtain a light and efficient boundary layer suction system become a key aspect of new active flow control concept for high lift.

While the research in the presented area is usually focused on maximizing lift coefficient, at the cost of high system requirements (such as the required pressure difference), the aim of this research is to look at the possible gains due to boundary layer suction on a multi-element airfoil while minimizing the power requirements for the boundary layer suction system.

The potential loss in the additional lift compared to one that could be obtained with a more demanding system should be compensated by a reduction in complexity, weight and the absence of the need for additional power for the new suction system. A passive system that has not been investigated so-far is sketched in fig. 1. In this case the low pressure area that exists in the flap tip area acts as the driver for the system. Whilst flow separation over the flap could be controlled with such a system it may also prove to be beneficial with respect to the flap end vortex development. Blowing inside or close to the vortex core potentially leads to a faster vortex decay that is attractive when requirements for separation distance due to wake vortex encounter is considered².

*Professor, Faculty of Aerospace Engineering, Delft University of Technology

†MSc Student, Faculty of Aerospace Engineering, Delft University of Technology

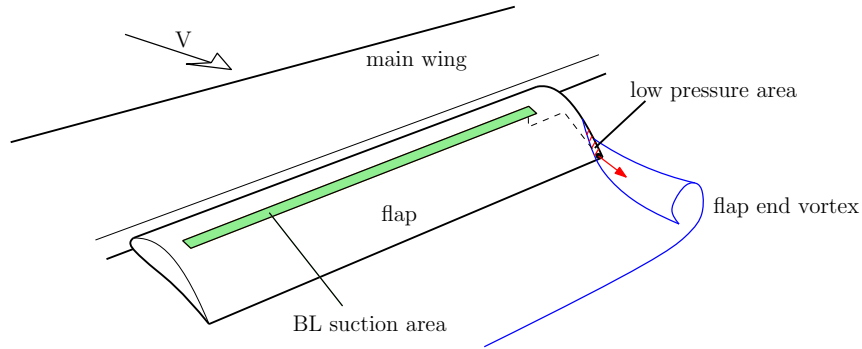


Figure 1. Conceptual drawing of a boundary layer suction system based on a flap end vortex low pressure area that drives the system. The sucked air is vented in the vicinity of the vortex core.

Before a system as sketched in fig. 1 could be designed an analysis of the potential gains in lift using BL suction was performed, the result of which is discussed in this paper. In order to perform this investigation the flow field is simulated with the inviscid-viscid interaction flow solver MSES which is suitable for multi-element airfoils. This code, denoted *MatSESSuction*, was adapted to include the simulation of boundary layer suction (BLS). The implementation of BLS relied heavily upon the work of Merchant⁵ and de Oliveira Andrade⁸ and mainly involved changing the integral boundary layer formulation and closure relations in MSES⁶.

The analysis of the changes to the high lift behavior were investigated based on a 2-dimensional flow analysis. Fig. 2 summarizes the key flow phenomena that can be distinguished³:

- Strongly curved boundary layers: static pressure can significantly vary throughout the boundary layer due to the large flow curvature.
- Compressible flow: the extremely high velocities over the first element. The slat in this case, can cause local supersonic velocities, even at free-stream Mach numbers in the order of $M = 0.2$.
- Recirculation zones: in cavities preceded by sharp edges a recirculation zone is formed.
- Relaminarization: due to the very strong favorable pressure gradient near the leading edge(s), turbulent boundary layers may relaminarize.
- Wakes: the exhausted or low-energy flow resulting from the boundary layers that leave an upstream element produces a wake that is influenced by downstream elements. Under influence of the adverse pressure gradient over downstream elements the wake may grow and merge with the boundary layer of a downstream element. Under influence of adverse pressure gradients the main element wake may experience flow reversal without being in contact with any surface. This is referred to as *wake bursting* or off-the-surface separation (in fig. 2 it is referred to as the ‘backflow region’).
- Separation: separation causes the flow field around the airfoil elements to break down with a major loss in lift as a result. In order to assess the flow field around a multi-element airfoil all these phenomena — or at least as much as possible — should be captured by the used method. Doing this computationally proves it to be extremely difficult to capture all these phenomena, and as a result predicting high-lift flows remains a challenging problem.

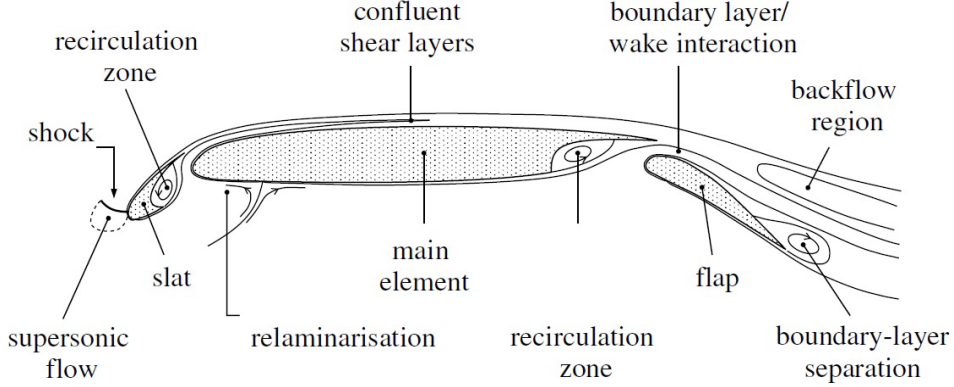


Figure 2. Phenomena influencing the flow over a multi-element airfoil³. This study concentrates on the flow reversal region that occurs in the free stream above the deflected flap.

II. Numerical suction model

A summary of the method applied to model the suction in the *MatSESSuction* program is provided here. Further details can be found in the work of van Craenenbroeck⁴. Starting point for the analysis performed herein is the MSES code of Drela⁶ which is an inviscid-viscid interaction aerodynamic solver which is able to solve aerodynamic flows around bodies which are ‘slender’ enough (i.e., no blunt bodies) for both subsonic and transonic flows and for high to relatively low Reynolds numbers.

The inviscid domain is solved by the Euler equations in conservative form:

$$\nabla \cdot \rho \mathbf{u} = 0 \quad (\text{continuity}) \quad (1)$$

$$\nabla \cdot (\rho \mathbf{u} \mathbf{u}^T) + \nabla p = 0 \quad (\text{momentum}) \quad (2)$$

$$\nabla \cdot (\mathbf{u}(E + \rho)) = 0 \quad (\text{energy}) \quad (3)$$

where ρ is the density, \mathbf{u} the flow speed, p the pressure and E the energy in the flow.

The solution for the viscous flow domain is obtained through the solution of three ordinary differential equations. These are the von Kármán momentum integral equation:

$$\frac{C_f}{2} = (H + 2 - M_e^2) \frac{\theta}{u_e} \frac{du_e}{d\xi} + \frac{d\theta}{d\xi} - C_\mu \quad (4)$$

The kinetic energy shape parameter equation:

$$\theta \frac{dH^*}{d\xi} + (H^{**} + H^*(1 - H)) \frac{\theta}{u_e} \frac{du_e}{d\xi} = (C_\mathfrak{D} + C_\mu) - H^* \left(\frac{C_f}{2} + C_\mu \right) \quad (5)$$

The shear lag equation:

$$\frac{\delta}{C_\tau} \frac{dC_\tau}{d\xi} = 4.2 \left(\sqrt{C_{\tau(eq)}} - \sqrt{C_\tau} \right) + \left(\frac{2\delta}{u_e} \frac{du_e}{d\xi} \right)_{(eq)} - \left(\frac{2\delta}{u_e} \frac{du_e}{d\xi} \right) \quad (6)$$

Here C_f is the friction coefficient, H the shape factor, θ momentum loss thickness, H^* the kinetic energy shape parameter, H^{**} the density shape parameter, $C_\mathfrak{D}$ the dissipation coefficient, C_τ the

shear stress coefficient and δ the boundary thickness. The streamwise coordinate in the BL is denoted by ξ . The conditions at the edge of the BL and at the wall are denoted by the indices e and w , respectively.

In eq. (4) and (5) the term C_μ , represents the effect of suction and it is defined as:

$$C_\mu = \frac{\rho_w v_w}{\rho_e u_e} \quad (7)$$

After discretization and linearization of the coupled, non-linear, Euler equations (1,2,3) combined with the viscous equations (4,5,6) a linear system of equations is obtained, represented by $F(\mathbf{U}) = 0$, where \mathbf{U} is the vector with the unknown variables.

The system of integral boundary layer equation is closed with so-called closure relations⁵. The inviscid and viscous domains are coupled by the well-known coupling condition that the displacement of the inviscid streamlines is proportional to the mass defect due to the presence of the boundary layer; an assumption which is acceptable for flows without massive separation. This mass defect equals $\rho_e u_e \delta^*$ and when no wall transpiration is present the displacement of the inviscid domain normal to the wall is simply equal to the displacement thickness itself:

$$\Delta n = \delta^* \quad (8)$$

The viscous and inviscid equations are simultaneously solved in the overall system of equations, hence they are ‘fully coupled’. The discretized and linearized system of equations is solved using the Newton method. For the process of determining the primary variables $n, \rho, C_\tau, \delta^*$ and θ , the reader is referred to van Craenenbroeck⁴ and de Oliveira Andrade⁸.

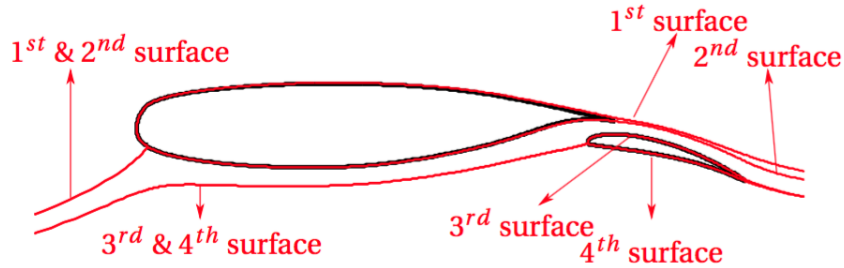


Figure 3. Boundary layer ‘surfaces’ as defined in MSES.

All BL variables tied to a certain grid node are stored in an array which will be referred to as a ‘BL surface’. Geometrically, these surfaces can be viewed as the equivalent inviscid streamlines for every element (for the upper and lower surface) as sketched in fig. 3. Also the suction distribution and, later on, $\delta_{suction}^*$, is read and stored into such a surface, which greatly simplifies the access to the correct suction value whenever necessary.

The well-known coupling condition of eq. (8) is compromised in the case of suction since a part of the mass in the boundary layer is sucked away and the displacement of the inviscid body, Δn , changes. Without suction, the mass defect is given by:

$$\dot{m}_{defect} = \rho_e u_e \delta^*$$

Taking into account the mass removed by suction this becomes (up to a point ξ_i along the BL):

$$\dot{m}_{defect} = \rho_e u_e \delta^* + \frac{1}{\rho_e u_e} \int_0^{\xi_i} \rho_w v_w d\xi \quad (9)$$

From eq. (9) it can be readily observed that Δn is dependent upon the solution for ρ_e and v_w . The addition of the second term on the right hand side of eq. (9) changes the resulting Jacobian that is used in the calculation of the solution vector, within the Newton method, drastically. As this task is not trivial it was decided to treat the integral as a constant during the Newton iteration and only change the right hand side to account for suction. In other words to assume that the solution process will not diverge when $\delta_{suction}^*$ is small enough. It turned out that this approach worked very well for the cases discussed herein⁴.

III. Validation of the suction model

A. Flat plate

In an experiment performed by Favre et al⁷ several boundary layer (BL) properties were measured for the flow over a flat plate for several suction quantities: $c_\mu = 0.000, 0.001, 0.005$ and 0.016 . The flow first travels over a flat plate without suction of 1026 mm , after which it continues over a perforated plate of 920 mm where suction can be applied. Transition occurs almost immediately at the leading edge. Simulating a flat plate in our solver, *MatSESuction* poses the problem of the leading edge of the plate: introducing corners at the leading edge will trigger separation, which is of course undesirable. A simple rounded edge avoids this, but will in turn introduce suction peaks influencing the start conditions for the boundary layer. Note that a convenient feature of the measurements by Favre et al is that the suction starts only approximately halfway the plate so the influence of the leading edge on the BL at the measurement location can remain limited. The flow is tripped at the leading edge of the plate in accordance with the experiment by Favre. The simulations were performed at a free-stream Reynolds number of approximately 7.5×10^5 and a Mach number of $M = 0.1$.

Fig. 4 shows the development of δ^* , θ and H over the perforated plate for several suction values. For the suction cases it can be seen that the displacement thickness and momentum thickness are generally slightly overpredicted by the code. Near the start of suction a peak in both δ^* and θ can be observed for the experimental data. However, it can be said with certainty that this is not related to the application of suction, but due to imperfections in the suction surface at this location (see⁷). The notably worse correlation for $c_\mu = 0.001$ and 0.005 is shown compared to the $c_\mu = 0.016$ case. No specific cause was found for this, so far.

B. Single element airfoil

A second validation of the *MatSESSuction* solver is done through a comparison with an earlier developed single element code, RFOILSUC, which is airfoil analysis code in which a suction model was implemented similar to the one in the current code. As such it is merely a check on the proper working and implementation of the suction model in the closure relations in *MatSESuction*.

The adaption and validation of RFOILSUC is described in de Oliveira Andrade⁸. The effect of suction on the skin friction coefficient and the momentum loss thickness is presented in fig. 5. As can be expected, the suction leads to a sharp rise in the skin friction coefficient. This is due to the ‘pulling’ effect of BLS. Very good agreement can be observed between the results of *MatSESuction* and RFOILSUC. Small differences can be attributed to a slight modeling difference: *MatSESuction* models the displacement of the inviscid region accounting for the mass defect in the BL due to suction, while RFOILSUC does not. The good agreement between the two codes is not a surprise however since the BL formulation and closure models are almost identical.

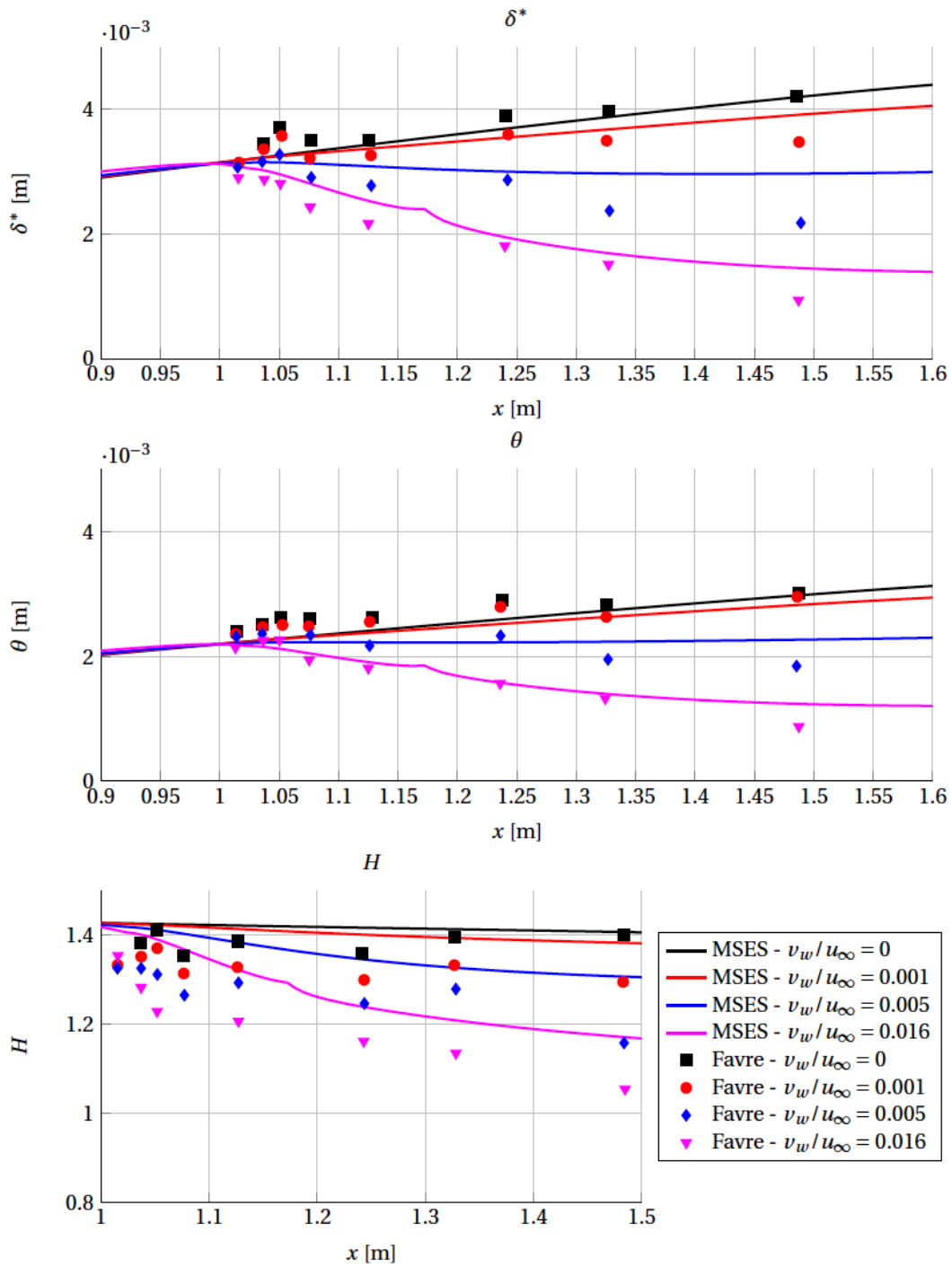


Figure 4. Boundary layer parameters from *MatSESuction* compared with Favre's experimental data⁷. Displacement thickness, δ^* , momentum loss thickness θ , and shape parameter, H .

The lift polars for the same configurations as those discussed above are compared in fig. 6, including experimental data for the non-suction case from Abott and Doenhoff⁹. Again, the agreement is very good, except for the region near $C_{l_{max}}$. *MatSESuction* struggles to converge to the right solution here, which is evidenced by the somewhat irregular shape of the lift polar in this area. Hence, our model should not be used at or close to maximum lift of the particular airfoil.

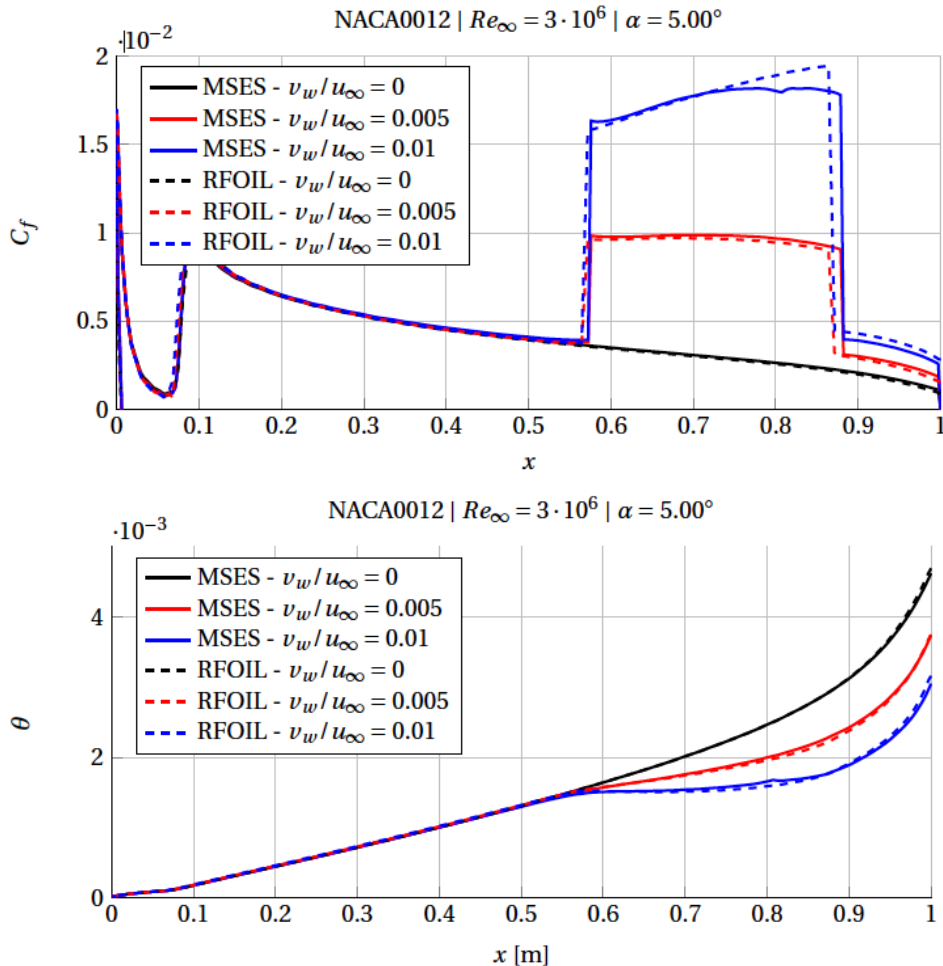


Figure 5. Comparison of the *MatSESuction* (denoted as MSES) and RFOILSUC (denoted as RFOIL) for the surface friction coefficient of a NACA0012 airfoil with suction. Experimental data taken from Abott and von Doenhoff⁹

IV. Wake in an adverse pressure gradient

As pointed out in various references the adverse pressure gradient effect on the wake of the main wing element may lead to off-the-surface flow reversal (often referred to as 'wake bursting') that seriously degrades the maximum lift. Smith¹⁰ already notes a lack of research on wake flow in an adverse pressure gradient in his classic paper on high lift aerodynamics. More recently additional references have become available on the topic. However, the vast majority of this research is a comparison between experimental and computational results¹¹⁻¹⁸. Since the computational sim-

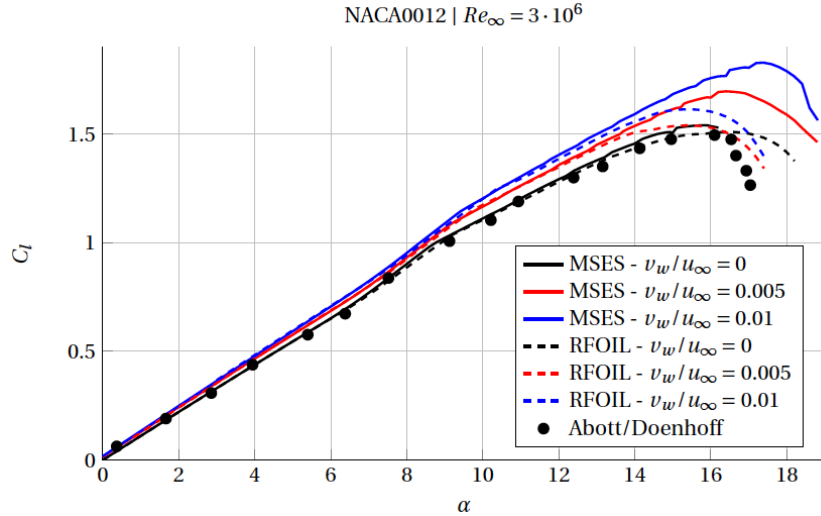


Figure 6. Comparison of *MatSESuction* (denoted as MSES) and *RFOILSUC* (denoted as RFOIL) for the lift polars of a NACA0012 airfoil with suction. Experimental data taken from Abott and von Doenhoff⁹

ulation of strongly ‘separated’ regions is difficult, these studies often only simulate only wakes in mild adverse pressure gradients. An exception to this is the study by Driver and Mateer¹⁹ in which results for adverse pressure high enough to create ‘massively separated regions’ off-the-surface. In this case that decambering of the entire flow field is so strong that it causes a significant loss of lift. The same strong effects due to wake bursting were found by Veldhuis et al²⁰ in an analysis of a modern high lift airfoil configuration.

In case of high lift systems whose performance is degraded due to wake bursting it becomes important to determine under which conditions flow separation becomes eminent. Gartshore’s criterion²¹ may be used determine whether a wake is growing or decaying, based on the observation that an adverse pressure gradient aggravates the momentum deficit and the viscous effect smooths it out. The criterion may be written as:

$$\frac{1}{1 - C_p} \frac{dC_p}{dx} > \frac{0.007}{\delta^*} \quad (10)$$

If the left-hand side of eq.(10) is less than $0.007/\delta^*$, the wake decays; if greater, it grows. Gartshore’s criterion relates the wake growth to a quantity that can directly be influenced by suction, namely the displacement thickness, δ^* . Hence, it is interesting to investigate in how far suction might help to allow larger adverse pressure gradient over the flap before wake bursting an the associated drop in lift can be postponed.

Fig. 7 shows the development of Gartshore’s criterion for the wakes of the NLR7301 airfoil with a deployed flap that is discussed in section V.A. In the left figure the geometry and (inviscid) streamlines are shown; the red band indicates boundary layer growth following Gartshore and the black band shows where there is actual boundary layer growth.

In the right figure the value of the criterion is shown along the trajectory of the wake (where it drops below zero there is wake growth). For the case $\delta_f = 28^\circ$ a large area of wake growth is predicted by Gartshore in the wake of the main element past the flap. However, in the figure on the right it can be seen that the criterion actually only marginally exceeds zero. This shows

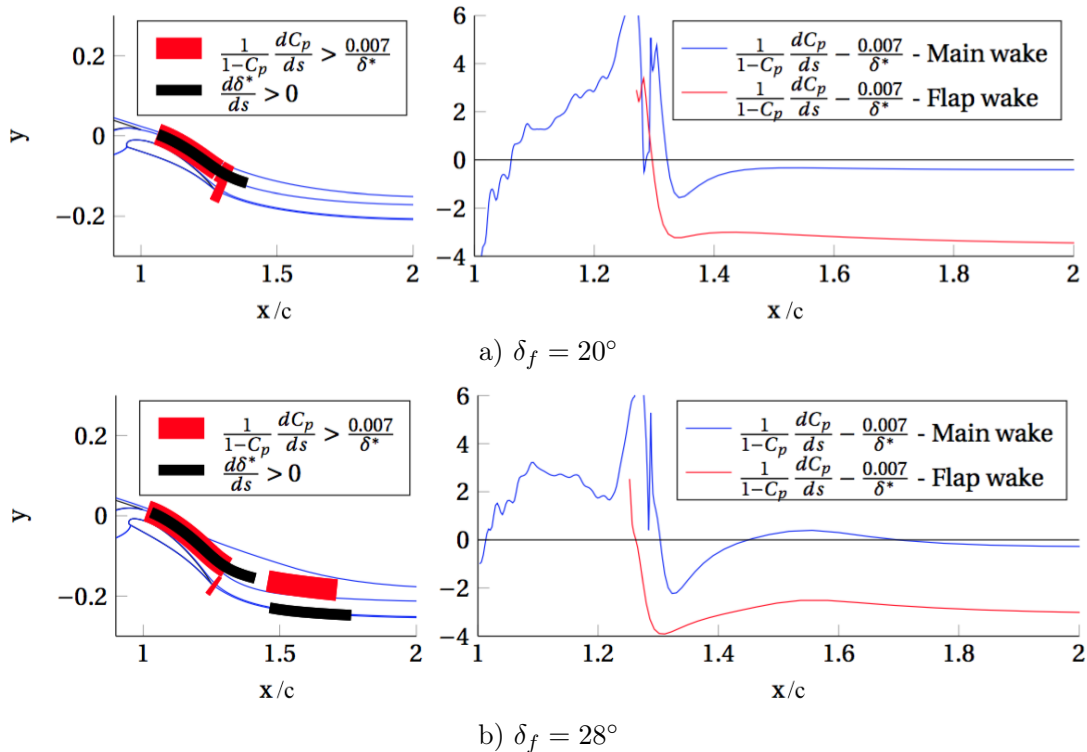


Figure 7. Comparison of wake growth according to Gartshore’s criterion and *MatSESuction* for a NLR7301 with deflected flap (see section V.A).

immediately one of the drawbacks of the criterion: while it may indicate wake growth, it does definitely not give very reliable information about the severity of it. The opposite is true for the wake of the flap: an area with wake growth is present that is not being picked up by Gartshore’s criterion; it should be said however that the wake growth is very small here. It is important to keep in mind that the criterion was actually developed from and for flow in the adverse pressure gradient over a flap; so further downstream it is probably not a valid model. In the region above the flap the results from Gartshore’s criterion follow the actual situation very well for all cases. Hence, the results of *MatSESuction* are reasonably well in line with Gartshore’s criterion. This strengthens the credibility of its predictive capabilities with respect to the wake’s behavior.

To determine the extent wake bursting it was decided that a good choice for a criterion, would be the rate at which the displacement thickness, δ^* grows⁴. At the onset of wake burst, the displacement effect of the wake will rapidly increase. The study by Driver and Mateer¹⁹ very conveniently presents three cases with no, mild and strong flow reversal. Before the onset of flow reversal, an almost linear increase in the displacement thickness can be observed for all three cases as shown in fig. 8. This allows to extract a constant spreading rate of the displacement thickness and link this spreading rate to a flow case with either a small or massive flow reversal.

V. Multi-element airfoil performance enhancement

To determine in how far the high lift performance of multi-element airfoils may be improved by postponing wake bursting through upper surface suction, two test cases were analyzed. The focus was to select the suction such that minimum pumping requirement would be attained, i.e. the suction area was positioned in a region with relatively high (yet negative) static pressure.

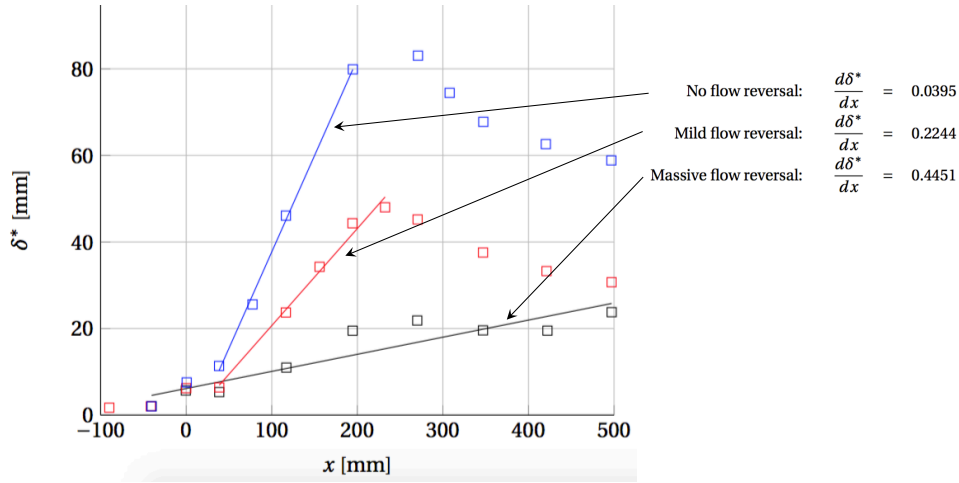


Figure 8. Displacement thickness spatial growth rates extracted from Driver and Mateer¹⁹.

A. NLR7301 with flap

The first example of a multi-element airfoil in which BLS was applied is the NLR7301 for which experimental data without suction were obtained by van den Berg and Oskam²². The airfoil geometry is shown in fig. 9.

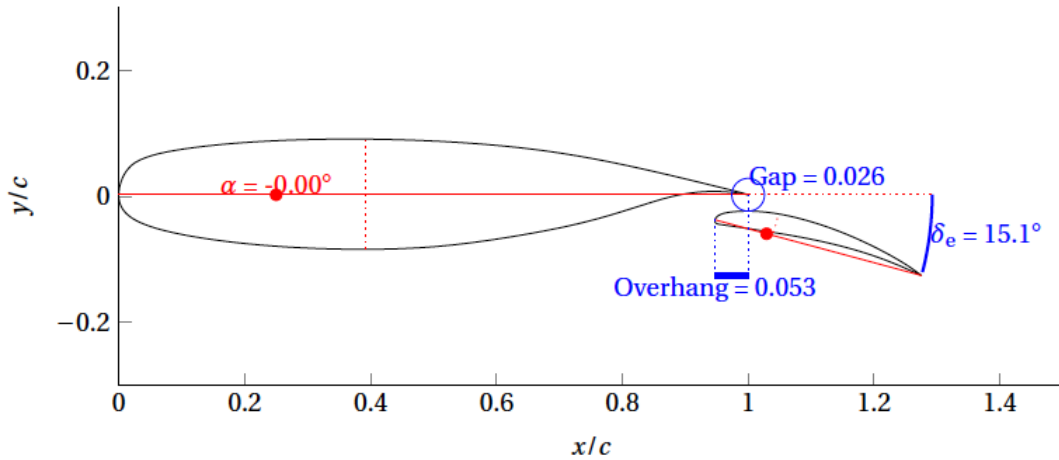


Figure 9. NLR7301 airfoil with flap layout²².

Fig. 10 shows the lift polar and the BL parameters δ^* and θ , for a Reynolds number of $Re = 2.51 \times 10^6$ and a Mach number $M = 0.185$. As can be seen the agreement is good quite good for the lift polar although prediction of $C_{l_{max}}$ remains troublesome, as expected. The decrease of δ^* over the part of the flap where there is a favorable pressure gradient and the sharp rise in the presence of an adverse pressure gradient is well predicted; only at the extremes the displacement thickness remains somewhat under-predicted. Also the momentum thickness shows good agreement, except for the last point at $x/c = 1.4$. The reason for this is not entirely clear, but it is suspected that interaction of the main element and flap wakes plays a role here, which is not predicted by *MatSESuction*.

Fig. 11 shows that at an angle of attack of 8° there is a change in the trend of the lift for flap deflections above $\delta_f = 24^\circ$. The spreading rate of the displacement thickness (fig. 11b) indicates

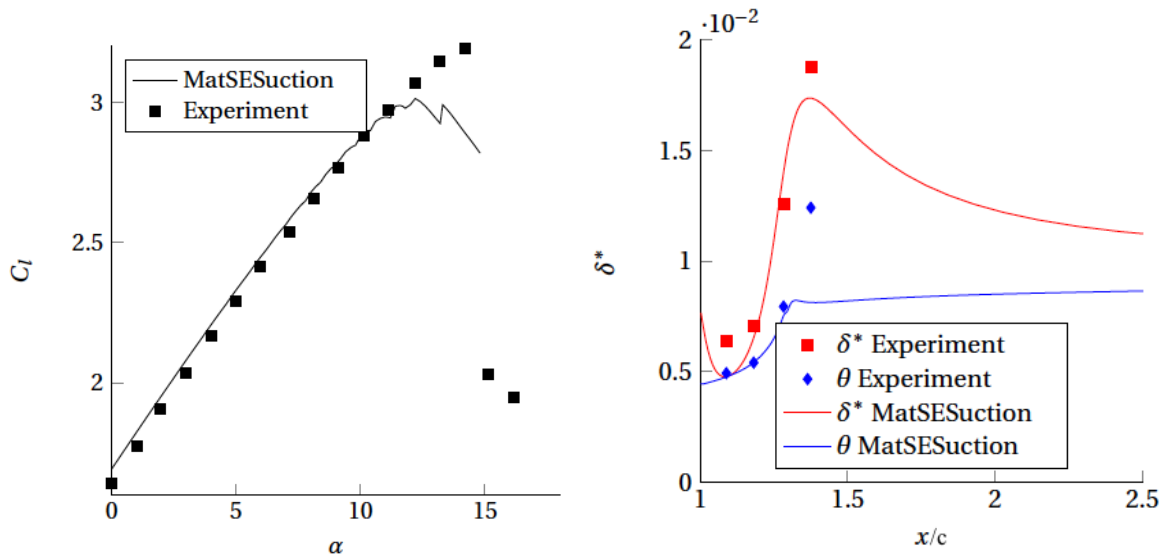


Figure 10. Comparison of experimental and calculated lift polar (left) and BL parameters for the NLR7301 model without suction²².

that the source of the problem is located in the wake: strong flow reversal is present here, or this is at least expected when comparing the spreading rate of δ^* with the critical values found from¹⁹.

The question is now whether the observed wake burst can be avoided by suction. To investigate this, suction was applied near the trailing edge from $x/c = 0.81$ to $x/c = 0.91$ with a strength of $v_w/U_\infty = -0.01$.

Fig. 12a shows the effect on the spreading rate of the displacement thickness for three configurations: two without suction and with the flap deflection of 24° and 28° respectively and one with suction, also with a flap deflection of 28° . The critical values for wake burst are also indicated. In this case a suction coefficient is used that is related to the airfoil chord:

$$C_q = -\frac{1}{U_\infty \rho_\infty c} \int \rho_w v_w d\xi \quad (11)$$

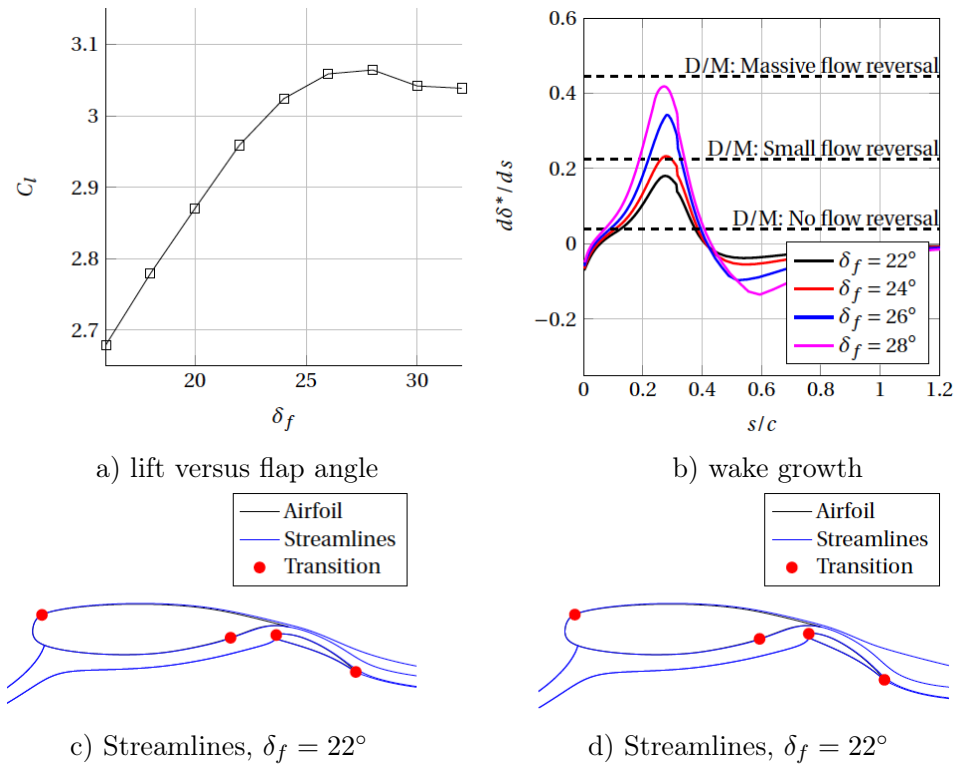
For a flap deflection of 24° and no suction the spreading rate of δ^* indicates that the wake is on the verge of bursting, but hasn't yet. No loss of lift is consequently observed in fig. 12b.

For $\delta_f = 28^\circ$ the critical value for $d\delta^*/ds$ has been well exceeded. This is also clear from the fact that the lift tops off for this flap deflection. Applying suction prevents the strong growth of the displacement thickness. This leads to a significant gain in lift: at a flap deflection of 28° the lift coefficient is increased from 3.064 to 3.196, which is increase of 4.3%.

B. MFFS026

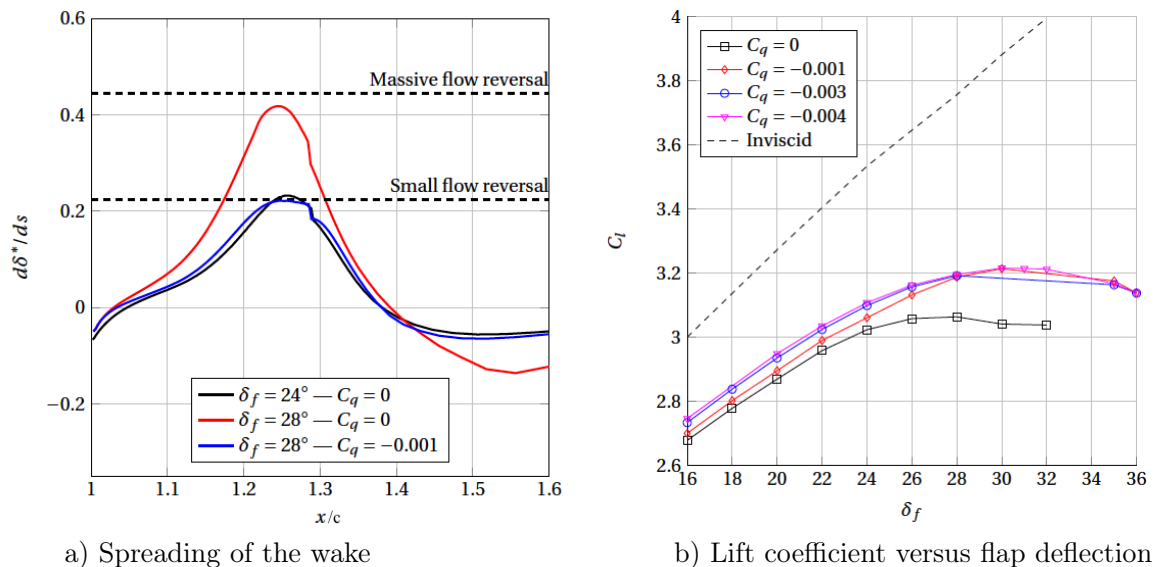
The MFFS026 airfoil is used specifically for the investigation of the wake burst phenomenon by Pomeroy et al¹¹. It is therefore also an interesting case to simulate in the context of this research. Fig. 13 shows the airfoil configuration. The flow around the airfoil system is nowhere stalled near the TE nor is there massive separation, or to put it with the words of Pomeroy et al. 'the flow is well behaved'; despite that the flow field does shown signs of the onset of wake burst. This is important since *MatSEsuction* cannot simulate flow regions with massive separation.

Concerning the wake, Pomeroy et al. report that bursting occurs in the main wake at $x/c \approx 0.96$ (and $y/c \approx -0.13$) and the flap wake at $x/c \approx 0.95$. Pomeroy et al. use a much more 'relaxed'



a) lift versus flap angle
b) wake growth
c) Streamlines, $\delta_f = 22^\circ$
d) Streamlines, $\delta_f = 22^\circ$

Figure 11. Calculated NLR7301 case without suction for $\alpha = 8^\circ$. Comparison of the wake growth for flap angles of $\delta_f = 22^\circ$ and $\delta_f = 28^\circ$, expressed in $d\delta^*/ds$ for which typical values were found in¹⁹ (denoted with D/M). Wake bursting is encountered for $\delta_f = 28^\circ$ in which case massive flow reversal in the outer flow above the flap is found.



a) Spreading of the wake
b) Lift coefficient versus flap deflection.

Figure 12. Calculated results for the NLR7301 model with suction. Spreading rate of the wake (a) and the lift coefficient vs. flap deflection for different suction rates (b). Suction allows higher flap deflections without a loss of lift by avoiding wake bursting.

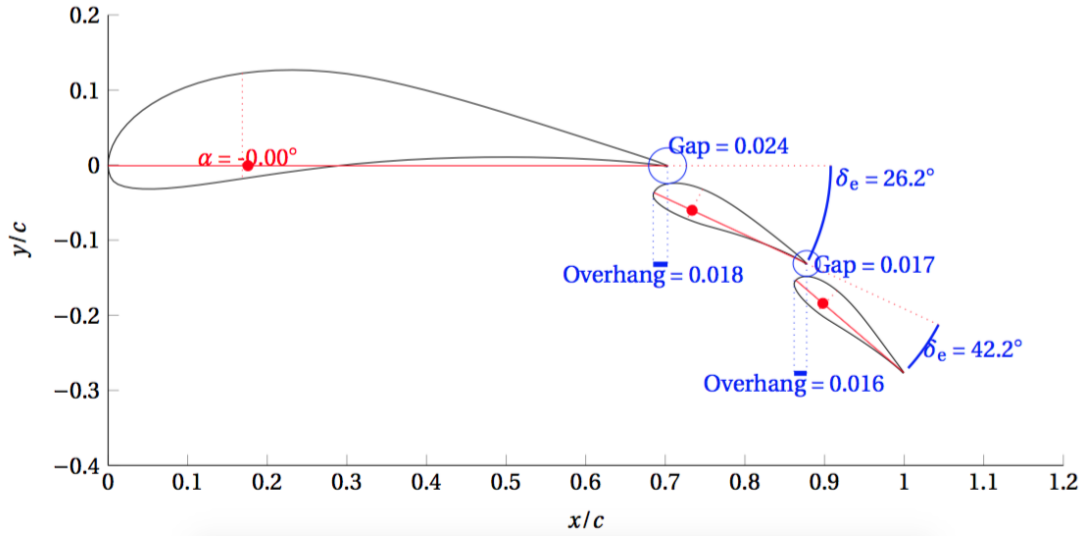


Figure 13. MFFS026 airfoil geometry¹¹

definition for wake burst, in the sense that not flow reversal or a loss of lift qualifies as ‘wake burst’, but merely rapid expansion of the wake and an increasing velocity deficit; in their case the wake core velocity only slows down to $0.7U_\infty$.

The ‘wake burst’ for the reference case of Pommery et al at $\alpha = 0^\circ$, discussed above, is very weak and it does not cause significant decambering of the flow yet. More interesting cases with respect to this can be found for larger flap deflections at higher angles of attack. Fig. 14 shows the variation of the lift coefficient with flap deflection at $\alpha = 12^\circ$.

The indicated flap deflection on the horizontal axis is that of the second flap; the first flap is always at a deflection of 16.5° less. Applying suction proves again to be successful in avoiding wake burst, as evidenced by fig. 15 as for a flap deflection of 45° , wake burst is avoided by applying suction between $x/c = 0.8$ to $x/c = 0.9$ with a wall velocity of only $v_w = -0.005$ ($C_q = -0.0005$).

As a result, the lift coefficient is increased from 3.5 to 3.6, or an increase of 3%. Increasing the suction level limits the spreading of the wake even further but only has a marginal effect on the eventual lift coefficient. For a larger flap deflection ($\delta_f = 47^\circ$) a higher suction level is necessary to lower the spreading rate of δ^* below the critical value; now this is only achieved for $C_q = -0.001$. The lift coefficient increases from 3.5 to 3.64 and 3.7 for $C_q = -0.0005$ and $C_q = -0.001$ respectively.

The comparison of the two flap angle cases 45° and 47° demonstrates nicely how increasing the suction level is only beneficial if it ‘pulls’ the spreading rate of the wake below the critical value of 0.23. This is also the reason why no suction was applied over the first flap: at no point the wake of the first flap comes close to the ‘danger zone’. Finally, fig. 16 presents the streamlines as calculated for $\alpha = 12^\circ$ and $\delta_f = 47^\circ$ case which clearly shows the beneficial effect of reducing the BL displacement thickness by applying the suction over the main element upper surface.

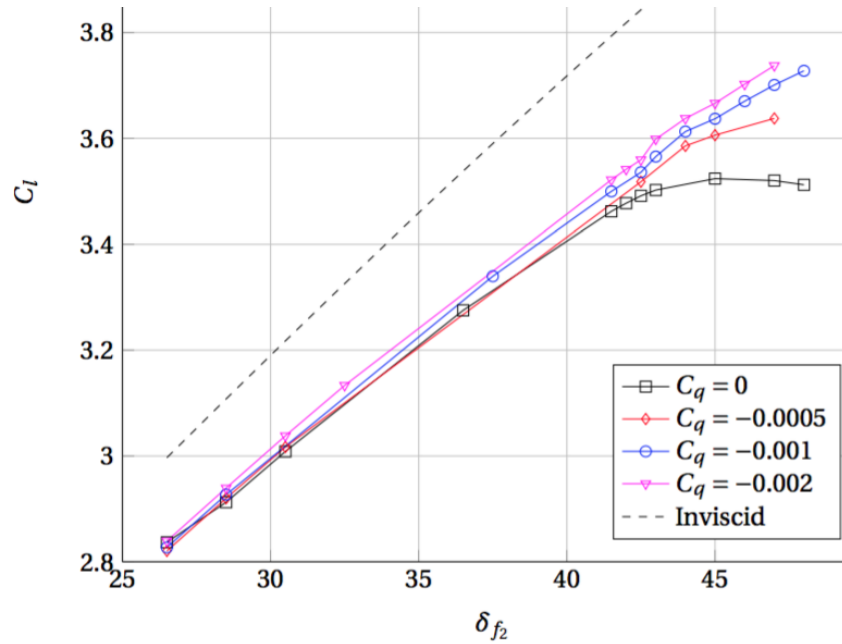


Figure 14. Lift coefficient vs. flap deflection for the MFFS026 airfoil at $\alpha = 12^\circ$. Without suction the lift tops off at $\delta_{f_2} = 45^\circ$, due to wake burst. This is however successfully prevented with suction which allows the lift to increase further with flap deflection.

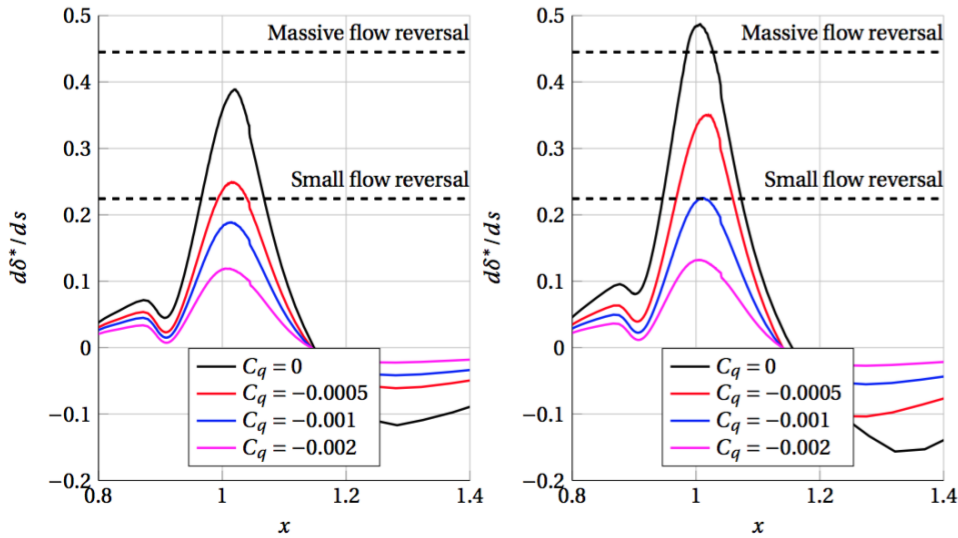


Figure 15. Spreading rate of δ^* for the MFFS026 airfoil at $\alpha = 12^\circ$ at $\delta = 45^\circ$ (left) and $\delta_f = 47^\circ$ (right). A suction level of $C_q = -0.0005$ is not sufficient to prevent wake burst which is also reflected in the lift that is obtained by this configuration.

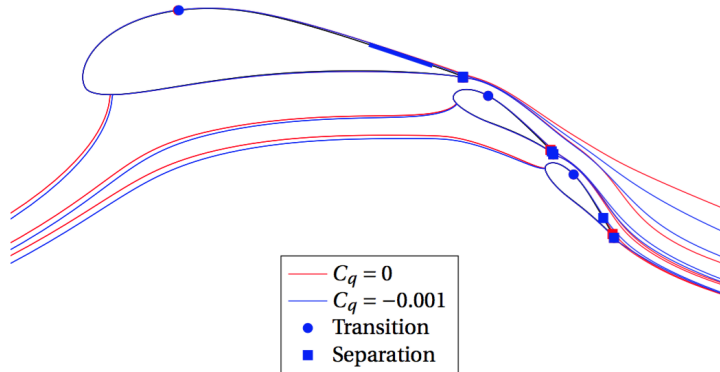


Figure 16. Streamlines around the MFFS026 airfoil at $\alpha = 12^\circ$ and $\delta_f = 47^\circ$ including an indication of the transition and separation points. Suction clearly limits the growth of the wake (this is especially true over the second element which is the critical location) which successfully increases the overall circulation.

VI. Conclusions

From this research on the effect of BL suction on the behavior on multi-element airfoils the following conclusions may be drawn:

- A boundary suction model was successfully implemented in the multi-element airfoil analysis code MSES. Apart from slot suction the effects of continuous suction over limited parts of the airfoil is well predicted, with the error for the suction cases in the same order as the non-suction case.
- The code, denoted *MatSESSuction*, was applied to flapped airfoils as a starting point to investigate possibilities for efficient (low power requirement) BL suction systems to improve high lift wings.
- To relax the requirements for large pressure differences over the suction area it is interesting to apply suction at a location with a relatively high static pressure. It was concluded that the most promising suction location is towards the trailing edge of an element to effectively influence the wake properties before entering the area with an adverse pressure gradient due to the flap.
- Making the boundary layer thinner with the help of suction can delay so-called wake bursting and increase the overall lift. Simulations on two typical multi-element airfoil systems in a configuration where wake bursting occurs, show that the overall lift can be successfully increased by approximately 4% through the application of suction of the main element. Only small suction rates were needed in this case.
- Additional analysis needs to be performed to determine the applicability of the method for mild to severe trailing edge flow separation control using BL suction. So far, this research has not provided definite conclusions on the possibility to apply local low surface pressure areas to drive the BL suction system without the need for additional power input to a suction pump.
- As is with all well known CFD models that are used for the prediction of the maximum lift coefficient, where significant flow separation occurs due to surface flow separation, the results are unreliable close to $C_{l_{max}}$ and vary from case to case. Therefore it is advisable to avoid using results in this flow regime.

References

- ¹J. Meister and J. Pfennig, Boundary layer suction arrangement, (2010), US Patent 7,837,155.
- ²T. Gerz, F. Holzapfel and D. Darracq, Commercial aircraft wake vortices. *Progress in Aerospace Sciences*, 38(3), 181–208, 2002
- ³M. Tummers, K. Hanjalić, D. Passchier, and R. Henkes, Computations of a turbulent wake in a strong adverse pressure gradient, *International Journal of Heat and Fluid Flow* 28, 418 (2007).
- ⁴J. van Craenenbroeck, Boundary layer suction configurations with minimal pump requirements for multi-element airfoils, MSc Thesis, Delft University of Technology, 2016
- ⁵A. A. Merchant, Design and analysis of supercritical airfoils with boundary layer suction, Master's thesis, Massachusetts Institute of Technology. Dept. of Aeronautics and Astronautics (1996).
- ⁶M. Drela, Two-Dimensional Transonic Aerodynamic Design and Analysis Using the Euler Equations, Phd thesis, Massachusetts Institute of Technology. Dept. of Aeronautics and Astronautics (1985).
- ⁷A. Favre, R. Dumas, and E. Verollet, Couche limite sur paroi plane poreuse, Tech. Rep. 39001554 (CEA Saclay, 91-Gif-sur-Yvette (France), Saclay, 1961).
- ⁸G. de Oliveira Andrade, Wind Turbine Airfoils with Boundary Layer Suction - A novel Design approach, Master's thesis, TU Delft, Delft University of Technology, Delft (2011).
- ⁹I. Abbott and A. Von Doenhoff, Theory of Wing Sections, Including a Summary of Airfoil Data, Dover Books on Aeronautical Engineering Series (Dover Publications, New York, 1959).
- ¹⁰A. M. O. Smith, High-Lift Aerodynamics, *Journal of Aircraft* 12, 501 (1975).
- ¹¹B.W. Pomeroy, J.M. Diebold, P. J. Ansell, and M. S. Selig, Study of Burst Wakes in a Multi-Element Airfoil Flowfield, *AIAA Journal* 52, 821 (2014)
- ¹²D. M. Driver and G. G. Mateer, Wake flow in adverse pressure gradient, *International Journal of Heat and Fluid Flow* 23, 564 (2002).
- ¹³A. Starke, R. Henkes, and M. Tummers, Effects of curvature and pressure gradient on a turbulent near wake, *Experimental Thermal and Fluid Science* 19, 49 (1999).
- ¹⁴R. Hoffenberg and J. Sullivan, Measurement and simulation of wake deceleration, in 36th AIAA Aerospace Sciences Meeting and Exhibit, Aerospace Sciences Meetings (American Institute of Aeronautics and Astronautics, 1998).
- ¹⁵G. Bucci, J. Sullivan, G. Bucci, and J. Sullivan, An experimental simulation of high lift wake flows at high Reynolds number, (American Institute of Aeronautics and Astronautics, 1997).
- ¹⁶F. O. Thomas and X. Liu, An experimental investigation of symmetric and asymmetric turbulent wake development in pressure gradient, *Physics of Fluids* 16, 1725 (2004).
- ¹⁷Fengjun Liu, William Liou, and Ronald Joslin, Numerical Simulations of Confluent Wake/Boundary Layer Flows, in 41st Aerospace Sciences Meeting and Exhibit, Aerospace Sciences Meetings (American Institute of Aeronautics and Astronautics, 2003).
- ¹⁸N. Duquesne, J. Carlson, C. Rumsey, and T. Gatski, Computation of turbulent wake flows in variable pressure gradient, in 30th Fluid Dynamics Conference, Fluid Dynamics and Co-located Conferences (American Institute of Aeronautics and Astronautics, 1999).
- ¹⁹D. M. Driver and G. G. Mateer, Wake flow in adverse pressure gradient, *International Journal of Heat and Fluid Flow* 23, 564 (2002).
- ²⁰L.L.M. Veldhuis, D.P. Jansen, J. El Haddar, G. Correale, Novel passive and active flow control for high lift, ICAS 2012-3.7.2, ICAS 2012 conference, Brisbane, Australia.
- ²¹I. Gartshore, Predictions of the blowing required to suppress separation from high lift airfoils, *CASI Transactions* 4, 39 (1971).
- ²²B. van den Berg and B. Oskam, Boundary layer measurements on a two-dimensional wing with flap and a comparison with calculations, in *AGARD Turbulent Boundary Layers* 14 p (SEE N80-27647 18-34), Vol. 1 (1980).